Structural Differences Between Wood Species: Evidence from Chemical Composition, FTIR Spectroscopy, and Thermogravimetric Analysis

Matheus Poletto,[1,2] Ademir J. Zattera,[2] Ruth M. C. Santana[1]

[1]*Laboratory of Polymeric Materials—Engineering School, Federal University of Rio Grande do Sul -UFRGS, Porto Alegre-RS-Brazil*
[2]*Laboratory of Polymers—Center of Exact Science and Technology, University of Caxias do Sul—UCS, Caxias do Sul-RS-Brazil*

Received 4 November 2011; accepted 10 February 2012
DOI 10.1002/app.36991
Published online in Wiley Online Library (wileyonlinelibrary.com).

ABSTRACT: In this study, the relationship between wood cellulose crystallinity, influence of extractives on wood degradation, correlation between chemical composition, and physical properties of four wood species were investigated by chemical analysis, Fourier transform infrared (FTIR) spectroscopy, and thermogravimetry. The chemical analysis showed that *Dipteryx odorata* and *Mezilaurus itauba* (ITA) contained a higher quantity of extractives and lower quantities of holocellulose and lignin than *Eucalyptus grandis* (EUG) and *Pinus elliottii*. FTIR spectroscopy indicated that higher extractives content in ITA might be associated with more intense bands at 2920, 2850, and 1510 cm^{-1}. The lower values for hydrogen bond energy and hydrogen bond intensity showed that EUG contained more absorbed water than the other species. Thermogravimetry confirm that lower extractive contents leads to a better wood thermal stability. This study showed that through the methods used previous information about structure and properties of wood can be obtained before use it in composite formulations. © 2012 Wiley Periodicals, Inc. J Appl Polym Sci 000: 000–000, 2012

Key words: wood, thermal stability; FTIR spectroscopy; thermogravimetry

INTRODUCTION

Wood is a natural composite consisting of cellulose, hemicellulose, and lignin, along with smaller quantities of extractives. Cellulose is a linear polymer of glucose units which can form intrachain and interchain bonds yielding a crystalline macromolecule[1] with higher molecular weight that the other wood components. The hydroxyl groups and their ability to form hydrogen bonds play a major role in directing the crystalline packing and also govern the physical properties of cellulose.[1] Hemicelluloses comprise a group of polysaccharides composed of a combination of 5- and 6-carbon ring sugars.[1] Hemicellulose have a more irregular structure with side groups, substituent groups, and sugars present along the length of the chain.[1,2] Lignin is a randomized condensed polymer with many aromatic groups and is much more hydrophobic than cellulose or hemicellulose.[2] Wood also contains a small amount of extractives, which can include lipids, phenolic compounds, terpenoids, fatty acids, resin acids, and waxes.[3] Generally, the extractives content varies between 2% and 5%, but it can be as high as 15%.[4]

The use of wood-based materials, such as wood flour and wood fibers, as reinforcement for thermoplastics has gained significant interest in recent years.[5–9] Wood offers a number of advantages over conventional reinforcing materials such as abundance, renewability, low-specific gravity, high-specific strength, and stiffness, and relatively low cost.[10] On the other hand, there are some drawbacks, such as a high level of moisture absorption, relatively low degradation temperatures around 200°C, and filler agglomeration because of the tendency of wood to form hydrogen bonds.[5,11] However, the relationship between the structural parameters, such as wood cellulose crystallinity, the influence of extractives content on wood degradation, and the correlation between the chemical composition and physical properties of wood are aspects that have not been fully explored. In order to better understand such relationships, the aim of this article was to establish the main structural differences between wood samples of different species through chemical analysis, Fourier transform infrared (FTIR) spectroscopy, and thermogravimetry analysis.

Correspondence to: M. Poletto (mpolett1@ucs.br).
Contract grant sponsor: CAPES.

TABLE I
Chemical Compositions of Wood Samples of the Species Investigated

Wood species	Holocellulose (%)	Lignin (%)	Extractives (%)	Ash (%)
Eucalyptus grandis (EUG)	62.7 ± 1.4	32.1 ± 1.0	4.1 ± 0.2	1.1 ± 0.3
Pinus elliottii (PIE)	61.2 ± 1.1	33.8 ± 1.0	4.5 ± 0.1	0.8 ± 0.1
Dipteryx odorata (DIP)	57.1 ± 0.6	30.4 ± 0.4	11.1 ± 0.1	1.5 ± 0.2
Mezilaurus itauba (ITA)	57.8 ± 1.0	28.0 ± 0.3	13.6 ± 0.7	0.7 ± 0.1

EXPERIMENTAL

Materials

The wood flour samples used in this study were obtained from wastes of the lumber industry in Brazil. The species investigated were *Pinus elliottii* (PIE), *Eucalyptus grandis* (EUG), *Mezilaurus itauba* (ITA), and *Dipteryx odorata* (DIP). The samples were dried at 105°C for 24 h in a vacuum oven before the tests. The average fiber particle length of the wood samples was around 200 μm.

Determination of wood components

Benzene and absolute ethanol, purchased from Vetec Chemical (Rio de Janeiro, Brazil), were used to determine the amount of organic extractives in the wood samples. Sulfuric acid, purchased from Vetec Chemical, was used for insoluble lignin determination. The wood extractives were eliminated from the samples via Soxhlet extraction in triplicate using: ethanol/benzene, ethanol, and hot water, according to the Tappi T204 cm-97 standard. The Klason lignin content was determined according to the Tappi T222 om-02 standard. The ash content was determined by calcination in a muffle furnace at 600°C for 1 h. The holocellulose content (cellulose + hemicellulose) was determined according to eq. (1)[12]:

$$\%\text{Holocellulose} = 100 - (\%\text{Lignin} + \%\text{Extractives} + \%\text{Ash}) \quad (1)$$

Fourier transform infrared (FTIR) spectroscopy

FTIR spectra were obtained on a Nicolet IS10-Thermo Scientific spectrometer. Wood powder samples of each species (5 mg) were dispersed in a matrix of KBr (100 mg), followed by compression to form pellets. The spectra were obtained using 32 scans, in the range of 4000 cm^{-1} to 400 cm^{-1}, at a resolution of 4 cm^{-1}. The magnitude FTIR spectra were normalized at 1435 cm^{-1}.[13] Second derivative spectra were obtained by applying the Savtzky–Golay function.

Thermogravimetric analysis

The thermogravimetric analysis (TGA50—Shimadzu) was carried out under constant nitrogen flow (50 mL/min), from 25 to 600°C, at a heating rate of 10°C/min. Approximately 10 mg of each sample was used.

RESULTS AND DISCUSSION

Wood components

The chemical compositions of the wood samples of the different species studied are showed in Table I. The holocellulose content was determined to be around 63% for EUG, 61% for PIE, and 57% for both DIP and ITA. However, ITA and DIP contain three times more extractives than EUG and PIE. The degradation temperature of a wood sample is expected to be related to the heat stability of the individual wood components.[3,14] Thus, differences in the thermal stability of wood samples from different species can be attributed to variations in the chemical composition and structure of the wood components.[15] The PIE had the highest lignin content with around 34% while ITA had the lowest at 28%. The ash content was quite similar for all wood samples studied.

The wood samples of the four species investigated have clearly distinguishable differences in their composition and differences in the structure of the wood components and the thermal behavior can therefore be expected.

FTIR spectroscopy

FTIR spectroscopy has been used as a simple technique for obtaining rapid information on the structure of wood constituents and chemical changes taking place in wood due to various treatments.[16,17] In contrast to conventional chemical analysis, this method requires small sample sizes, short analysis time, and does not destroy the wood structure.[2]

Because of their complexity, the spectra were separated into two regions, namely: the OH and CH stretching vibrations in the 3800–2700 cm^{-1} region (Fig. 1) and the "fingerprint" region which is assigned to stretching vibrations of different groups of wood components at 1800–800 cm^{-1} (Fig. 3). The FTIR spectra and second derivative spectra for the different wood samples studied in the region of 3800–2700 cm^{-1} are shown in Figure 1(a,b), respectively. It can be observed in Figure 1(a) that there is a strong broad band at around 3400 cm^{-1} which is

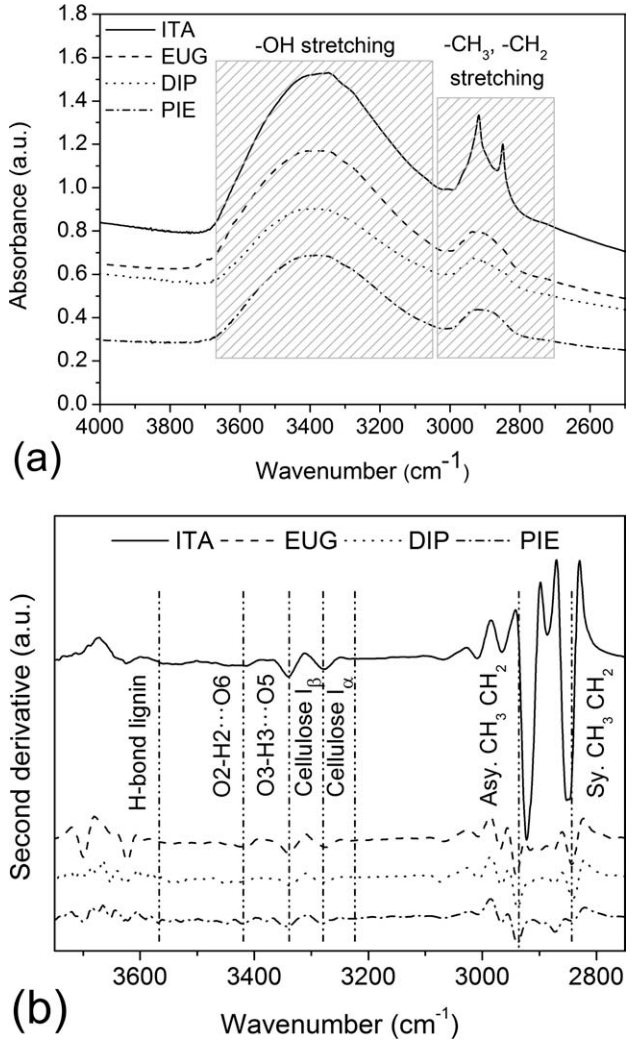

Figure 1 FTIR spectra (a) and the second derivative spectra (b) of the wood samples studied O(2)H-O(6)(intra), O(3)H-O(5) (intra), O(6)H-O(3′)(inter).

assigned to different O—H stretching modes and another two bands at around 2920 and 2850 cm^{-1} related to asymmetric and symmetric methyl and methylene stretching groups present in the spectra of all of the wood components but most notably in the spectra for cellulose,[18,19] shown in detail in Figure 1(b). However, these two bands are more prominent in the ITA spectra at 2916 and 2852 cm^{-1}, respectively. This might be attributed to the higher extractives content in this wood, since some compounds in organic extractives, like fatty acid methyl esters and phenolic acid methyl esters, contain methyl and methylene groups.[20–22]

According to the literature,[2,23] there are intermolecular and intramolecular H-bonds in cellulose I and in lignin. In cellulose I a secondary OH group at the C3 position forms an H-bond with an O5 atom of the adjacent ring (O3—H3···O5 intramolecular H-bond), and another secondary OH group at the C2 position forms an H-bond with an O6 atom

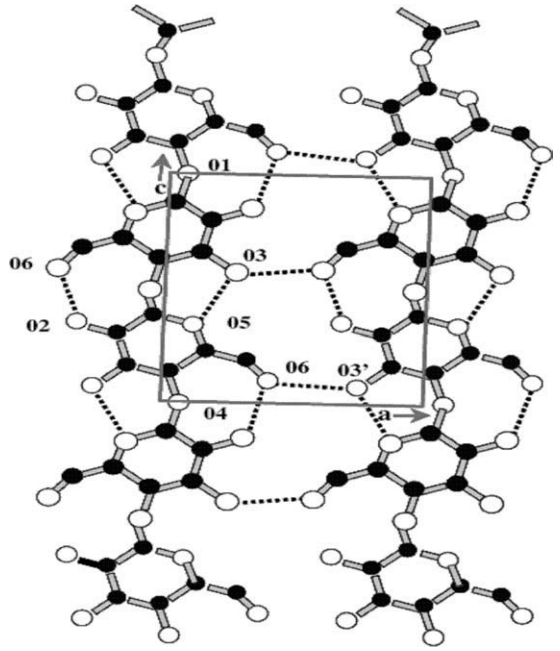

Figure 2 Proposed hydrogen-bonding in cellulose I/cellulose II by Kolpak and Blackwell (Oh et al.,[23]).

of the adjacent ring (O2—H2···O6 intramolecular H-bond). A primary OH group in the C6 position is involved in an H-bond with an O3 atom in the neighboring chain (O6—H6···O3′ intermolecular H-bond), as can be seen in Figure 2. Also, aliphatic hydroxyl groups in lignin have the potential to form stronger intermolecular hydrogen bonds than phenolic hydroxyl groups.

$$O(2)H\text{—}O(6)(\text{intra}), O(3)H\text{—}O(5)(\text{intra}), O(6)H\text{—}O(3')(\text{inter})$$

The hydroxyl stretching region is particularly useful for elucidating hydrogen-bonding patterns. However, the bands described below can generally be seen only in the second derivative of the FTIR spectra, which normally enhance the apparent resolution and amplify small differences in the FTIR spectrum.[2] Figure 1(b) shows the main bands in this region. Each distinct hydroxyl group in this region gives a single stretching band at a frequency that decreases with increasing strength of the hydrogen-bonding. These H-bonds are considered to be responsible for various properties of native cellulose, lignin, and, of course, wood itself.[2,23] Thus, the closer the cellulose chains the greater the interaction between the adjacent chains, resulting in more and stronger H-bonds which can lead to greater packing of cellulose chains and an increase in the strength of wood.

The intramolecular hydrogen bond in a phenolic group in lignin is observed at around 3568–3577 cm^{-1}.[17] In cellulose, an intramolecular hydrogen

TABLE II
The Energy of the Hydrogen Bonds and Hydrogen Bond Distance for Wood Samples Studied

	3567 cm^{-1}		3423 cm^{-1}		3342 cm^{-1}		3278 cm^{-1}		3221 cm^{-1}	
Wood species	E_H (kJ)	R (Å)	E_H (kJ)	R (Å)	E_H (kJ)	R (Å)	E_H (kJ)	R (Å)	E_H (kJ)	R (Å)
Eucalyptus grandis (EUG)	6.185	2.832	16.182	2.800	22.438	2.782	26.574	2.768	30.349	2.756
Pinus elliottii (PIE)	6.329	2.831	16.757	2.799	22.007	2.782	26.394	2.768	30.314	2.757
Dipteryx odorata (DIP)	6.401	2.831	16.613	2.799	22.438	2.781	26.610	2.768	30.874	2.754
Mezilaurus itauba (ITA)	6.473	2.831	16.325	2.800	22.295	2.781	26.753	2.767	30.493	2.756

bond vibration, derived from O2—H2···O6, appears at around 3432 cm^{-1}.[23,24] The frequencies for the O3—H3···O5 intramolecular hydrogen bond in cellulose normally occur at 3342 cm^{-1}.[24] The two characteristic bands assigned to the two crystalline cellulose allomorphs, cellulose I_α, and cellulose I_β, also occur in the region of 3220–3280 cm^{-1}.[2] A very small peak, normally shifted to lower wavenumbers, at 3221 cm^{-1} was attributed to hydrogen bonds only in cellulose I_α.[2,23] The band at 3221 cm^{-1} is assigned to the O6—H6···O3 intramolecular hydrogen bonds present only in triclinic I_α cellulose, whereas the band at close to 3277 cm^{-1} is proportional to the amount of monoclinic cellulose I_β.

The energy of the hydrogen bonds E_H for several OH stretching bands has been calculated using eq. (2)[25]:

$$E_H = \frac{1}{k}\left[\frac{(v_o - v)}{v_o}\right] \quad (2)$$

where ν_o is the standard frequency corresponding to free OH groups (3650 cm^{-1}), ν is the frequency of the bonded OH groups, and k is a constant ($1/k = 2.625 \times 10^2$ kJ).

The energy of hydrogen bonds are presented in Table II where it can be observed that they are very similar; however, the energy of the hydrogen bond for EUG at 3567 cm^{-1} shows a small decrease when compared with the other species. This could be associated with a higher quantity of absorbed water in the structure of EUG, since the band at 3567 cm^{-1} is assigned to the weakly absorbed water in free OH(6) and OH(2).[24,26,27]

The hydrogen bond distances R are obtained using the Pimentel and Sederholm equation as follows[28]:

$$\Delta v(cm^{-1}) = 4430 \times (2.84 - R) \quad (3)$$

where $\Delta\nu = \nu_o - \nu$, ν_o is the monomeric OH stretching frequency, which is taken to be 3600 cm^{-1}, and ν is the stretching frequency observed in the infrared spectrum of the sample. The hydrogen bond distances of the samples are quite similar for the species studied at all wavenumbers considered, as can be seen in Table II. Also, these values are close to that obtained by Popescu et al.[18]

In the "fingerprint" region, the spectra contain several bands assigned to the main wood components, as can be seen in Figure 3. The bands at 1595, 1510, and 1270 cm^{-1} are assigned to C=C, C—O stretching or bending vibrations of different groups present in lignin. The bands at 1460, 1425, 1335, 1220, and 1110 cm^{-1} are characteristic of C—H, C—O deformation, bending, or stretching vibrations of many groups in lignin and carbohydrates. The bands at 1735, 1375, 1240, 1165, 1060, 1030 cm^{-1} are assigned to C=O, C—H, C—O—C, C—O deformation or stretching vibrations of different groups in carbohydrates.[18,26]

The band at 1735 cm^{-1} is assigned to C=O stretching vibrations of the carboxyl and acetyl groups in hemicellulose.[18,26] Higher holocellulose content is indicated by a strong and broad band at 1735 cm^{-1}.[29] The EUG shows a more prominent band than the other three wood at 1736 cm^{-1}, in agreement with the highest content of holocellulose observed for this species, see Table I. The absorption peak at 1510 cm^{-1} arising from the aromatic skeletal vibration C=C of the benzene ring is characteristic of lignin.[26,29] For this band, the ITA and DIP species presented the most prominent band indicating higher lignin content than the EUG and PIE species,

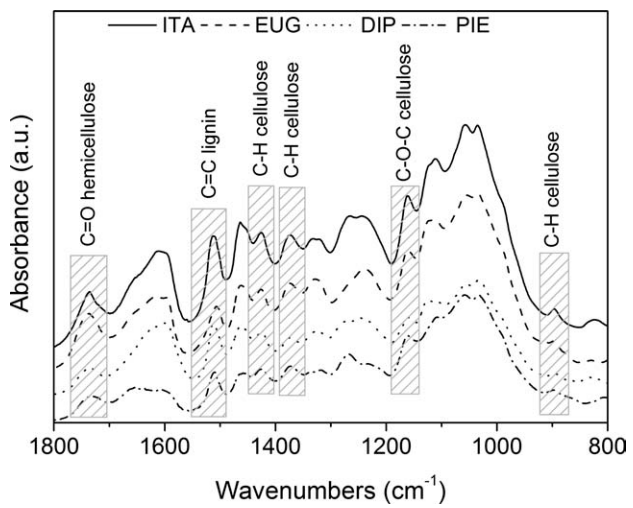

Figure 3 FTIR spectra in the 1800–800 cm^{-1} region.

according to Figure 3. However, the chemical method used to determine the wood components presented in Table I revealed that EUG and PIE contain more lignin than ITA and DIP. A probable explanation for this fact is that ITA and DIP contain around three times more extractives that EUG and PIE and some compounds of the extractives might be absorbed at around 1510 cm^{-1}. An example of this is the benzoic acids presents in wood tannins[20] that contain aromatic rings in their structure, and since the absorption at 1510 cm^{-1} is assigned to C=C stretching of the aromatic ring this may influence the intensity of this band. Pandey (2005)[30] observed in wood samples which contain a much higher amount of organic extractives that these compounds have a significant contribution to the 1510 cm^{-1} peak. Therefore, great care needs to be taken when using the peak at 1510 cm^{-1} to compare the different lignin contents and lignin/carbohydrate ratios in wood samples from species with higher contents of extractives.

The band at 1420–1430 cm^{-1} is related to aromatic skeletal vibrations associated with C—H in plane deformation of cellulose.[31] The bands at 1372 cm^{-1} and 1160 cm^{-1} are bands characteristic of carbohydrates. The band at 1375 cm^{-1} is assigned to CH bending in cellulose and hemicellulose while the band at 1165 cm^{-1} is assigned to C—O—C asymmetric stretching vibrations in cellulose and hemicellulose.[13] The band at 898 cm^{-1} is assigned to CH deformation in cellulose.[13,23] The band at around 1420–1430 cm^{-1} is designated as associated with the amount of crystalline structure of the cellulose, while the band at 898 cm^{-1} is assigned to the amorphous region in cellulose.[13] The ratio between the two bands was defined as an empirical crystallinity index proposed by Nelson and O'Connor (1964)[32] as a lateral order index (LOI). The ratio between the bands at 1372 cm^{-1} and 2900 cm^{-1}, proposed by Nelson and O'Connor (1964)[32] to be the total crystalline index (TCI), was used to evaluate the infrared crystallinity (IR) ratio. Considering the chain mobility and bond distance, the hydrogen bond intensity (HBI) of cellulose is closely related to the crystal system and the degree of intermolecular regularity, that is, crystallinity, as well as the amount of bound water.[31] The ratio between the absorbance bands at 3400 and 1320 cm^{-1} was used to study the HBI of the wood samples of the different species. The band at 1320 cm^{-1} is assigned to the CH_2 rocking vibration in cellulose.[26] The results obtained are presented in Table III.

The TCI is proportional to the degree of crystallinity of cellulose.[33] in wood and the LOI is correlated to the overall degree of order in the cellulose.[33,34] EUG showed the highest TCI and LOI values indicating the highest degree of crystallinity and a more ordered cellulose structure than the other species. On the other hand, ITA presented the lowest TCI and LOI values which may indicate that the cellulose of this wood is composed of more amorphous domains when compared with the other three species evaluated, while PIE and DIP presented intermediate values. Another interesting finding is that DIP presented a high LOI value, similar to that of EUG, which is associated with a lateral ordered cellulose structure. The crystallinity of the cellulose in wood is closely related to the thermal stability of the wood.[35,36] Therefore, it is possible that wood samples with higher TCI and LOI values have a greater thermal stability. However, EUG had the lowest HBI value. This result may be associated with a greater amount of absorbed water in the EUG wood, since the HBI value also represents the amount of absorbed water.[31] This is in agreement with EUG having the lowest value for the hydrogen bond energy at 3567 cm^{-1} which is assigned to the weakly absorbed water on free OH(6) and OH(2),[24,26,27] see Table II. The PIE sample had the highest HBI value while DIP and ITA presented similar values.

TABLE III
Infrared Crystallinity Ratio and Hydrogen Bond Intensity for the Wood Sample

Wood species	IR crystallinity ratio H1372/H2900 (TCI)	IR crystallinity ratio H1429/H897 (LOI)	HBI A3400/A1320
Eucalyptus grandis (EUG)	0.608	3.172	1.440
Pinus elliottii (PIE)	0.474	2.299	1.598
Dipteryx odorata (DIP)	0.389	3.137	1.508
Mezilaurus itauba (ITA)	0.237	2.060	1.523

Thermogravimetric analysis

The thermal stability of wood flour used as a filler or reinforcement in polymer matrix composites is of paramount importance.[14,37] The manufacturing of composites requires the mixing of lignocellulosic materials and the polymer matrix at temperatures of around 200°C for the most common thermoplastic polymers.[11,37] The degradation of wood due to high temperatures at the time of processing may lead to undesirable properties, such as odor and browning, along with a reduction in mechanical properties.[3,14] Hence, it is imperative that the degradation profile of wood flour is determined prior to its use in composite applications.[37] The thermal analysis curves for the wood samples of the four different species studied are presented in Figure 4.

Figure 4(a) gives the weight loss as a function of temperature, while Figure 4(b) presents the derivative thermogravimetric curves. All curves show a

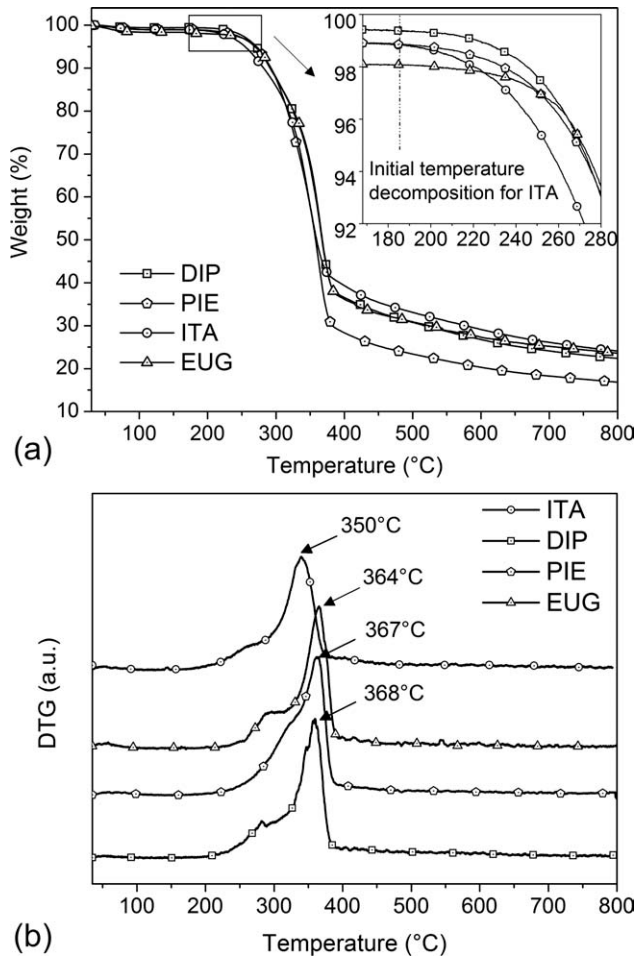

Figure 4 TGA (a) and DTG (b) curves for the wood species studied.

small weight loss below 100°C, which can be attributed to the evaporation of water. After this small weight loss, the degradation process occurs as a two-step process. In the first step, the degradation of hemicellulose takes place at around 300°C and a slight shoulder in the DTG curve can be seen in Figure 4(b) for all wood species studied. At around 350–370°C the main degradation of cellulose occurs and a prominent peak appears at the temperature corresponding to the maximum decomposition rate. According to Kim et al. (2006),[38] the depolymerization of hemicellulose occurs between 180 and 350°C, the random cleavage of the glycosidic linkage of cellulose between 275 and 350°C, and the degradation of lignin between 250 and 500°C.

As can be seen in detail in Figure 4(a), at temperatures around 180°C the ITA wood shows a more significant weight loss. This behavior might be associated with the highest content of extractives being found in this wood, around 14%, as seen in Table I. Extractives are compounds with lower molecular mass, when compared to cellulose, that can promote ignition of the wood at lower temperatures as a result of their higher volatility and thus accelerate the degradation process. Thus, the degradation of one wood component may accelerate the degradation of the others. However, the wood of DIP, which contains around 11% of extractives, showed higher thermal stability than ITA. This behavior may be related to the higher content of lignin in DIP than in ITA.

Wood is commonly used as filler in polymers processed at temperatures around 200°C.[3,11] Accounting to this fact, ITA and PIE woods initiate a more pronounced degradation process at around 180–190°C and 190–200°C, respectively. The low degradation temperature of ITA and PIE samples can lead to undesirable composite properties when processed at temperatures above 200°C. On the other hand, DIP and EUG woods initiate a more pronounced degradation process at around 220°C which can lead to thermoplastic polymer composites with higher mechanical and thermal properties by increasing the processing temperature range.

The EUG presented a slightly more pronounced weight loss at lower temperatures, around 2% at 100°C. This finding may be associated with the absorbed water in the EUG wood structure, corroborating the lower values for the hydrogen bond energy at 3567 cm^{-1} and hydrogen intensity, see Tables II and III. However, due to the high content of holocellulose and lignin, the most pronounced weight loss of the EUG wood starts at around the same temperature as that for the PIE wood, as can be seen in detail in Figure 4(a).

The initial weight loss temperature, T_i, of all samples, considered as the temperature at which the sample looses 3% of its weight, as shown in Table IV. ITA presented the lowest T_i value, as can be seen in detail in Figure 4(a). This may be associated with higher volatility of extractives and hemicellulose in this wood. The highest T_i values were observed for the EUG, PIE, and DIP wood species. On the other hand, EUG, ITA, and DIP had a significant amount of residue at 800°C probably due to higher inorganic contents in these three wood species.

All samples showed a shoulder at around 300°C associated with the main degradation of hemicellulose.[39] This shoulder is better evinced for the ITA,

TABLE IV
Thermal Degradation Temperatures and Residue at 800°C for the Wood Species Studied

Wood species	T_i (°C) 3 wt % loss	T shoulder (°C)	DTG peak (°C)	Residue at 800°C (%)
Eucalyptus grandis (EUG)	250	291	364	23.6
Pinus elliottii (PIE)	251	322	367	16.8
Dipteryx odorata (DIP)	257	289	368	22.4
Mezilaurus itauba (ITA)	237	275	350	24.1

EUG, and DIP wood species, as can be seen in Figure 4(b). For PIE the shoulder occurs at a higher temperature than for the other wood species. This result may be a consequence of lower extractives volatility and lower hemicellulose reactivity. The main degradation of cellulose occurs at higher temperatures for EUG, PIE, and DIP respectively. For EUG the main degradation temperature of cellulose occurs at 364°C and might be related to the higher content of holocellulose and lower content of extractives in this wood, see Table I. For ITA wood the main degradation of cellulose occurs at 350°C, around 14°C lower than the EUG wood, in agreement with the degradation of one component with lower molecular weight, such as the extractives, may accelerate the degradation process of the other wood components, such as the cellulose. This confirms the higher crystallinity of the cellulose in EUG when compared to ITA, indicated by the highest TCI and LOI values observed for EUG in Table III, which increases the thermal stability of wood.

The amount of DIP extractives is higher while the content of holocellulose is lower than those of EUG and PIE. However, the thermal stability was more pronounced and the main decomposition of cellulose was higher for DIP as compared to EUG and PIE. This behavior may be associated with the highest LOI of cellulose in this wood. The more ordered cellulose chains in this wood species may be caused by higher thermal stability.

Wood is an anisotropic material and its decomposition is a complex process. It may be difficult to distinguish and model the thermal decomposition behavior of each specific component in wood due to the complexity of growth of wood which causes variance in components content, crystal structure, and chemical composition from one species to another.[14,39,40]

CONCLUSIONS

In conclusion, the three methods used to characterize wood samples of four different species were found to be appropriate to evaluate differences in the structures of wood components. The chemical analysis revealed that the wood samples of the DIP and ITA species contain a higher quantity of extractives and a lower quantity of holocellulose and lignin than EUG and PIE. In the FTIR spectroscopy analysis, it was observed that the higher extractives content in ITA wood might be associated with the prominent bands at 2920, 2850, and 1510 cm^{-1}, indicating that care needs to be taken when using these bands to compare the different lignin contents and lignin/carbohydrate ratios of wood samples with higher extractives contents. The lower values for the hydrogen bond energy at 3567 cm^{-1} and hydrogen intensity indicate that the EUG wood contained more absorbed water than the samples of the other species and the thermogravimetric analysis confirmed this result. The thermogravimetric results confirmed that higher quantities of holocellulose, higher crystallinity, a more ordered cellulose structure, and higher quantities of lignin associated with a lower content of extractives lead to wood with a better thermal stability.

The authors acknowledge Prof. Ricardo Campomanes for supplying the wood samples of *Mezilaurus itauba* and *Dipteryx odorata*.

References

1. John, M. J.; Thomas, S. Carbohydr Polym 2008, 71, 343.
2. Popescu, M.-C.; Popescu, C.-M., Lisa, G.; Sakata, Y. J Mol Struct 2011, 988, 65.
3. Shebani, A. N.; van Reenen, A. J.; Meincken, M. Thermochim Acta 2008, 481, 52.
4. Zhang, X.; Nguyen, D.; Paice, M.; Tsang, A.; Renaud, S. Enzyme Microb Technol 2007, 40, 866.
5. Nachtigall, S. M. B.; Cerveira, G. S.; Rosa, S. M. L. Polym Test 2007, 26, 619.
6. Adhikary, K. B.; Pang, S.; Staiger, M. P. Compos B 2008, 39, 807.
7. Kim, J.-W.; Harper, D. P.; Taylor, A. M. J Appl Polym Sci 2009, 112, 1378.
8. Ashori, A.; Nourbakhsh, A. Bioresour Technol 2010, 101, 2515.
9. Poletto, M.; Dettenborn, J.; Zeni, M.; Zattera, A. J. Waste Manage 2011, 31, 779.
10. Bengtsson, M.; Le Baillif, M.; Oksman, K. Compos A 2007, 38, 1922.
11. Araújo, J. R.; Waldman, W. R.; De Paoli, M. A. Polym Degrad Stab 2008, 93, 1770.
12. Rowell, R. Handbook of Wood Chemistry and Wood Composites; CRC Press: Boca Raton, 2005.
13. Åkerholm, M.; Hinterstoisser, B.; Salmén, L. Carbohydr Res 2004, 339, 2889.
14. Poletto, M.; Dettenborn, J.; Pistor, V.; Zeni, M.; Zattera, A. J. Mater Res 2010, 13, 375.
15. Marcovich, N. E.; Reboredo, M. M.; Aranguren, M. I. Thermochim Acta 2001, 372, 45.
16. Chen, H.; Ferrari, C.; Angiuli, M.; Yao, J.; Raspi, C.; Bramanti, E. Carbohydr Polym 2010, 82, 772.
17. Popescu, C.-M.; Popescu, M.-C.; Vasile, C. Carbohydr Polym 2010, 82, 362.
18. Popescu, C.-M.; Singurel, G.; Popescu, M.-C.; Vasile, C.; Argyropoulos, D. S.; Willför, S. Carbohydr Polym 2009, 77, 851.
19. Adel, M. A.; Abb El-Wahab, Z. H.; Ibrahim, A. A.; Al-Shemy, M. T. Carbohydr Polym 2011, 83, 676.
20. Yokoi, H.; Nakase, T.; Goto, K.; Ishida, Y.; Ohtani, H.; Tsuge, S.; Sonoda, T.; Ona, T. J Anal Appl Pyrolysis 2003, 67, 191.
21. Ishida, Y.; Goto, K.; Yokoi, H.; Tsuge, S.; Ohtani, H.; Sonoda, T.; Ona, T. J Anal Appl Pyrolysis 2007, 78, 200.
22. Mészáros, E.; Jakab, E.; Várhegyi, G. J Anal Appl Pyrolysis 2007, 98, 61.
23. Oh, S. Y.; Yoo, D. I.; Shin, Y.; Kim, H. C.; Kim, H. Y.; Chung, Y. S.; Park, W. H.; Youk, J. H. Carbohydr Res 2005, 340, 2376.
24. Kondo, T. Cellulose 1997, 4, 281.
25. Struszczyk, H. J Mol Sci A 1986, 23, 973.
26. Schwanninger, M.; Rodrigues, J. C.; Pereira, H.; Hinterstoisser, B. Vib Spectrosc 2004, 36, 23.

27. Popescu, C.-M.; Popescu, M.-C.; Singurel, G.; Vasile, C.; Argyropoulos, D. S.; Willför, S. Appl Spectrosc 2007, 61, 1168.
28. Pimentel, G. C.; Sederholm, C. H. J Chem Phys 1956, 24, 639.
29. Pandey, K. K. J Appl Polym Sci 1999, 71, 1969.
30. Pandey, K. K. Polym Degrad Stab 2005, 87, 375.
31. Oh, S. Y.; Yoo, D. I.; Shin, Y.; Seo, G. Carbohydr Res 2005, 340, 417.
32. Nelson, M. L.; O'Connor, R. T. J Appl Polym Sci 1964, 71, 1311.
33. Carrilo, F.; Colom, X.; Suñol, J. J.; Saurina, J. Eur Polym J 2004, 40, 2229.
34. Corgié, S. C., Smith, H. M.; Walker, L. P. Biotechnol Bioeng 2011, 108, 1509.
35. Kim, U.-J.; Eom, S. H.; Wada, M. Polym Degrad Stab 2010, 95, 778.
36. Poletto, M.; Pistor, V.; Zeni, M.; Zattera, A. J. Polym Degrad Stab 2011, 96, 679.
37. Tserki, V.; Matzinos, P.; Kokkou, S.; Panayiotou, C. Compos A 2005, 36, 965.
38. Kim, H.-S.; Kim, S.; Kim, H.-J.; Yang, H.-S. Thermochim Acta 2006, 451, 181
39. Yao, F., Wu, Q., Lei, Y., Guo, W.; Xu, Y. Polym Degrad Stab 2008, 93, 90.
40. Di Blasi, C. Prog. Energy Combust Sci 2008, 34, 47.